

Robust Commutation Design: Applied to Switched Reluctance Motors

Max van Meer¹, Gert Witvoet^{1,2}, Tom Oomen^{1,3}

Abstract—Switched Reluctance Motors (SRMs) are cost-effective electric actuators that utilize magnetic reluctance to generate torque, with torque ripple arising from unaccounted manufacturing defects in the rotor tooth geometry. This paper aims to design a versatile, resource-efficient commutation function for accurate closed-loop control of a range of SRMs, mitigating torque ripple despite manufacturing variations across SRMs and individual rotor teeth. The developed commutation function optimally distributes current between coils by leveraging the variance in the torque-current-angle model and is designed with few parameters for easy integration on affordable hardware. Monte Carlo simulations and experimental results show a tracking error reduction of up to 31% and 11%, respectively. The developed approach is beneficial for applications using a single driver for multiple systems and those constrained by memory or modeling effort, providing an economical solution for improved tracking performance and reduced acoustic noise.

I. INTRODUCTION

Switched Reluctance Motors (SRMs) have gained industrial interest due to their compelling advantages in energy efficiency, simplicity of design, and lack of permanent magnets, especially for low-cost applications that involve mass production [1], [2]. The working principle of SRMs involves the controlled switching of currents to different coils to produce magnetic attraction, a process that, if carried out imperfectly, can give rise to torque ripple.

Torque ripple is a common challenge in the implementation of SRMs, and it has a range of different causes such as sampling [3], magnetic hysteresis [4] and magnetic saturation [5], and the most important is imperfect commutation. The mechanism through which currents are applied to different coils to produce torque is specified by a user-defined commutation function [3], [6], [7], [8]. The design of such a function relies on a model of the torque-current-angle relationship of the SRM. Any mismatch between this simplified model and the true system leads to a position-dependent error between the desired torque and the achieved torque, degrading the tracking performance of the

system. Reasons for model mismatch include manufacturing tolerances and assembly variations.

The rotor of an SRM features a large number of teeth, each of which is slightly different due to imperfections in the manufacturing process, resulting in significant tooth-dependency in the torque-current-angle relationship of an SRM [9, Chapter 5], see Figure 1. Similarly, in mass production, manufacturing tolerances lead to variations in the rotor teeth across different SRMs as well. Modeling all these variations across teeth and SRMs requires a tremendous effort when compared to using a commutation function which is designed using a low-order model of only one ‘average’ tooth. Indeed, in low-cost applications that involve mass production, it is economically desirable to ship each SRM with the same driver for commutation, each of which has sufficient memory to store the torque-current-angle relationship of only one average tooth.

Torque ripple is inevitable when variations across teeth or SRMs are ignored for economic reasons, and yet the magnitude of the torque ripple is affected by the choice of the commutation function, see Figure 2. At the same time, there is a high degree of design freedom in the design of commutation functions [3], because multiple coil currents together lead to a single torque on the rotor. It is therefore hypothesized that there exists a low-order commutation function that mitigates torque ripple across many teeth and SRMs while relying on a low-order model of only one average tooth.

Measurement data should be exploited to understand how manufacturing defects affect the torque-current-angle relationship of SRMs. In, [10], a data-driven identification approach for the torque-current-angle relationship of SRMs is presented that yields accurate SRM models for use in commutation design, without relying on separate dedicated torque sensors. Importantly, this method not only yields an estimated model but also the variance of the model parameters. This variance reflects the variation that arises from tooth-by-tooth variations, or, when data from different SRMs is used, SRM-to-SRM variations.

Although existing approaches to commutation function design are effective in the presence of a perfect model of every single tooth for each SRM, these methods lead to significant torque ripple in case of model mismatch due to manufacturing defects. To require detailed, high-order models of SRMs defeats the purpose of using an SRM in many low-cost applications, not only because this requires expensive modeling effort, but also because it leads to high requirements on the driver hardware. Therefore, this paper

¹Max van Meer (e-mail: m.v.meer@tue.nl), Gert Witvoet and Tom Oomen are with the Control Systems Technology section, Department of Mechanical Engineering, Eindhoven University of Technology, The Netherlands. This work is part of the research programme VIDI with project number 15698, which is (partly) financed by the Netherlands Organisation for Scientific Research (NWO). In addition, this research has received funding from the ECSEL Joint Undertaking under grant agreement 101007311 (IMOCO4.E). The Joint Undertaking receives support from the European Union’s Horizon 2020 research and innovation programme.

²Gert Witvoet is also with the Department of Optomechatronics, TNO, Delft, The Netherlands.

³Tom Oomen is also with the Delft Center for Systems and Control, Delft University of Technology, Delft, The Netherlands.

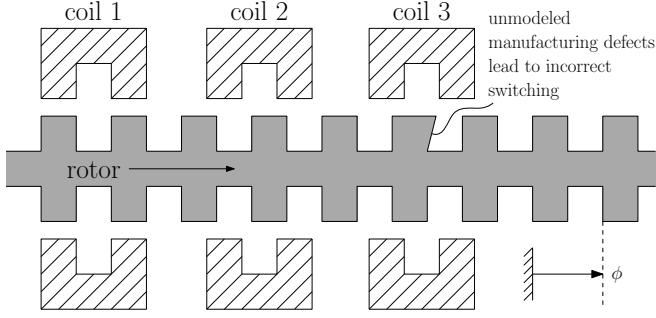


Fig. 1. Schematic overview of an SRM with three coils. Sequentially applying currents to the coils attracts rotor teeth, generating torque. When control designs involve commutation functions that rely on incorrect or incomplete models, torque ripple occurs, degrading tracking performance.

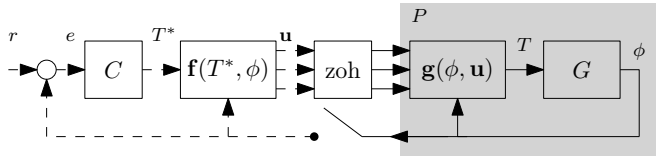


Fig. 2. Control scheme for an SRM P : The SRM's nonlinear dynamics are linearized using a commutation function \mathbf{f} to achieve $\hat{\mathbf{g}}\mathbf{f} = \pm 1$, enabling the use of a linear feedback controller $C(z)$. Solid lines and dashed lines depict continuous-time and discrete-time signals, respectively.

aims to develop a universal, resource-efficient commutation function that leverages the available information of the model variance to reduce torque ripple across different rotor teeth and SRMs. This is achieved by using the parameter variance matrix resulting from [10] to pose an optimization problem that minimizes the expected norm of the anticipated torque ripple. Moreover, the optimization-based framework for commutation function design from [3] is adopted, making it straightforward to include other desirable properties in the optimization problem, such as power consumption or constrained slew rates.

The contributions of this paper are therefore threefold:

- C1: A method for the design of robust commutation functions is developed. By solving a convex optimization problem that penalizes the expected value of the anticipated torque ripple, a commutation function is obtained that leads to the best performance for the average tooth or SRM, despite unknown manufacturing defects.
- C2: A Monte Carlo study is performed to show that the implementation of a single robust commutation function on a range of mass-produced, slightly different SRMs, results in increased tracking performance compared to conventional commutation functions.
- C3: Experimental validation results show that the robust commutation functions mitigate torque ripple caused by tooth-by-tooth variations on a single SRM.

This paper is structured as follows. In Section II, the problem formulation is given. Next, in Section III, the design method is detailed. Subsequently, the results are presented in Section IV, and finally, conclusions are drawn in Section VI.

II. PROBLEM FORMULATION

In this section, the problem formulation is given. First, the nonlinear dynamics of Switched Reluctance Motors are explained. Next, the control of SRMs is described, and finally, the problem definition of robust commutation design is given.

A. Dynamics of Switched Reluctance Motors

Switched Reluctance Motors (SRMs) are characterized by a nonlinear relationship between torque, current, and rotor angle. Figure 1 provides a schematic illustration of an SRM. In the absence of magnetic saturation, an SRM with n_t teeth and n_c coils is modeled as:

$$T_c(\phi, i_c) = \frac{1}{2} \frac{dL_c(\phi)}{d\phi} i_c^2, \quad (1)$$

where T_c represents the torque applied to the rotor by magnetizing coil $c \in \{1, \dots, n_c\}$ with a current i_c . $L_c(\phi)$ denotes the phase inductance, which varies periodically with the rotor position ϕ , having a spatial period of $\frac{2\pi}{n_t}$. Both the torque T and inductances L_c are unmeasured and hence unknown. The total torque applied to the rotor at time t is

$$T(t) = \mathbf{g}(\phi(t))\mathbf{u}(t), \quad (2)$$

where $\mathbf{g}(\phi)$ is defined as:

$$\mathbf{g}(\phi) := \frac{1}{2} \frac{d}{d\phi} [L_1(\phi(t)), \dots, L_{n_c}(\phi(t))], \quad (3)$$

and $\mathbf{u}(t)$ represents the squared coil currents:

$$\mathbf{u}(t) := [i_1^2(t), \dots, i_{n_c}^2(t)]^\top. \quad (4)$$

The following section addresses how a desired torque T^* is realized, using a model $\hat{\mathbf{g}} \approx \mathbf{g}$.

B. Commutation: linearization of SRM dynamics

To achieve a desired torque T^* in SRMs, we invert the nonlinear torque-current-angle relationship (2) through a commutation function $\mathbf{u} = \mathbf{f}(\phi, T^*)$ as follows. First, \mathbf{f} is structured as

$$\mathbf{f}(\phi, T^*) := \begin{cases} \mathbf{f}^+(\phi)T^* & T^* \geq 0, \\ -\mathbf{f}^-(\phi)T^* & T^* < 0, \end{cases} \quad (5)$$

where $\mathbf{f}^+(\phi), \mathbf{f}^-(\phi) : \mathbb{R} \rightarrow \mathbb{R}^{n_c}$ are functions that are designed to satisfy

$$\hat{\mathbf{g}}(\phi)\mathbf{f}^+(\phi) \approx 1, \quad \hat{\mathbf{g}}(\phi)\mathbf{f}^-(\phi) \approx -1, \quad (6)$$

such that when \mathbf{f}^+ or \mathbf{f}^- is multiplied with a desired torque T^* , the resulting currents lead to $T \approx T^*$, see (2). Moreover, as \mathbf{f} produces squared currents, it must be ensured that

$$\mathbf{f}^+(\phi) \geq \mathbf{0}, \quad \mathbf{f}^-(\phi) \geq \mathbf{0}. \quad (7)$$

It is important to note that multiple functions $\mathbf{f}(\phi, T^*)$ satisfy these requirements due to \mathbf{g} and \mathbf{f} being row and column vector functions, respectively. By applying the control law

$$\mathbf{u}(t) = \mathbf{f}(\phi(t), T^*(t)), \quad (8)$$

the squared currents for each coil to achieve the desired torque T^* are determined, as visualized in Figure 2. Combined with (2), the resulting torque is:

$$T(\phi(t)) = \mathbf{g}(\phi(t))\mathbf{f}(\phi(t), T^*(t)), \quad (9)$$

or equivalently,

$$T(\phi(t)) = b^\pm(\phi(t)) T^*, \quad (10)$$

with

$$\begin{aligned} b^\pm(\phi) &:= \mathbf{g}(\phi)\mathbf{f}^\pm(\phi), \\ \hat{b}^\pm(\phi) &:= \hat{\mathbf{g}}(\phi)\mathbf{f}^\pm(\phi). \end{aligned} \quad (11)$$

Here, $\pm := \text{sign}(T^*)$, e.g., \mathbf{f}^\pm refers to either \mathbf{f}^+ or \mathbf{f}^- , depending on the sign of T^* . Additionally, $b^\pm(\phi)$ denotes the true relative torque mismatch T/T^* while $\hat{b}^\pm(\phi)$ represents the expected mismatch, which is approximately ± 1 as per design, see (6).

Ideally, if the model is perfect, i.e., $\hat{\mathbf{g}}(\phi) = \mathbf{g}(\phi)$, and \mathbf{f} meets the requirements in (6), the realized torque matches the desired torque for all rotor positions ϕ . However, if $\hat{\mathbf{g}}(\phi) \neq \mathbf{g}(\phi)$, torque ripple occurs, degrading the tracking performance [11]. The next subsection defines the problem of designing commutation functions \mathbf{f} that counteract such model imperfections.

C. Problem definition

Our purpose is to design a commutation function $\mathbf{f}(\phi, T^*)$, structured as in (5), that mitigates torque ripple arising from modeling errors $\hat{\mathbf{g}}(\phi) \neq \mathbf{g}(\phi)$. Specifically, the objective is to minimize the true relative torque error

$$\begin{aligned} \varepsilon_T^\pm(\phi) &:= b^\pm(\phi) \mp 1, \\ &= \mathbf{g}(\phi)\mathbf{f}^\pm(\phi) \mp 1, \end{aligned} \quad (12)$$

where $\mp := -\text{sign}(T^*)$. The following cost function is considered:

$$\begin{aligned} \mathcal{J} &= \|\varepsilon_T^+(\phi)\|_{2,\Phi}^2 + \|\varepsilon_T^-(\phi)\|_{2,\Phi}^2, \\ \text{with } \Phi &= \{\phi \mid 0 \leq \phi < 2\pi\}. \end{aligned} \quad (13)$$

Since \mathbf{g} is unknown, the modeling error $\varepsilon_T^\pm(\phi)$ is unknown, so this cost function cannot be evaluated directly. Therefore, it is assumed that the model $\hat{\mathbf{g}}(\phi, \boldsymbol{\theta})$ with parameters $\boldsymbol{\theta} \in \mathbb{R}^{n_\theta}$ is probabilistic, indicating that some information about the modeling errors is available. More precisely, $\boldsymbol{\theta}$ is a multivariate Gaussian with

$$\boldsymbol{\theta} \sim \mathcal{N}(\hat{\boldsymbol{\theta}}, \boldsymbol{\Sigma}_\theta). \quad (14)$$

Identification of $\hat{\boldsymbol{\theta}}$ and $\boldsymbol{\Sigma}_\theta$ is addressed in [10]. In this paper, $\hat{\boldsymbol{\theta}}$ and $\boldsymbol{\Sigma}_\theta$ are assumed to be known, with $\hat{\boldsymbol{\theta}}$ generally unequal to $\boldsymbol{\theta}_{\text{true}}$ and $\boldsymbol{\Sigma}_\theta$ positive definite. The objective is then to minimize the following cost function:

$$\begin{aligned} \hat{\mathcal{J}} &= \mathbb{E} [\|\hat{\varepsilon}_T^+(\phi)\|_{2,\Phi'}^2 + \|\hat{\varepsilon}_T^-(\phi)\|_{2,\Phi'}^2], \\ \text{with } \Phi' &= \{\phi \mid 0 \leq \phi < 2\pi/n_t\}, \end{aligned} \quad (15)$$

where Φ' spans only a single tooth because we desire a resource-efficient commutation function that is the same

for every tooth, using a model $\hat{\mathbf{g}}(\phi, \boldsymbol{\theta})$ that is also tooth-invariant, albeit probabilistic. In the next section, the the model variance $\boldsymbol{\Sigma}_\theta$ is exploited in the design of \mathbf{f} , to minimize torque ripple arising from modeling errors $\hat{\mathbf{g}}(\phi, \boldsymbol{\theta}) \neq \mathbf{g}(\phi)$.

III. ROBUST COMMUTATION FUNCTION DESIGN

This section elaborates on the approach developed for designing robust commutation functions. First, the chosen model structures of the SRM model and the commutation functions are derived. Next, the expected torque ripple is expressed in terms of the uncertain model and the commutation function. Finally, the optimization problem is presented.

A. Parametrization of commutation functions and dynamics

The given SRM model, denoted by $\hat{\mathbf{g}}(\phi, \boldsymbol{\theta})$, as well as the commutation functions $\mathbf{f}^\pm(\phi, \boldsymbol{\alpha})$, are both parametrized linearly in their parameters. The structure of the provided SRM model is given by

$$\hat{\mathbf{g}}^\top(\phi, \boldsymbol{\theta}) = \boldsymbol{\psi}_g(\phi)\boldsymbol{\theta}, \quad (16)$$

where $\boldsymbol{\psi}_g : \mathbb{R} \rightarrow \mathbb{R}^{n_c \times n_\theta}$ serves as the basis of $\hat{\mathbf{g}}(\phi, \boldsymbol{\theta})$. Similarly, the commutation functions \mathbf{f}^+ and \mathbf{f}^- are parametrized as follows. Both \mathbf{f}^+ and \mathbf{f}^- are designed with n_α parameters per coil, i.e., $\alpha_{c,i}^+$ and $\alpha_{c,i}^-$ denote the i^{th} parameter of coil $c \in \{1, \dots, n_c\}$ of commutation functions \mathbf{f}^+ and \mathbf{f}^- respectively. We then define \mathbf{f}^+ and \mathbf{f}^- as

$$\mathbf{f}^\pm(\phi) = \boldsymbol{\psi}_f(\phi)\boldsymbol{\alpha}^\pm, \quad (17)$$

where $\boldsymbol{\alpha}^\pm = [\alpha_1^\pm, \dots, \alpha_c^\pm, \dots, \alpha_{n_c}^\pm]^\top$ stacks the parameters of all coils, $\alpha_c^\pm = [\alpha_{c,1}^\pm, \dots, \alpha_{c,n_\alpha}^\pm]^\top$ are the parameters of a single coil c , and

$$\boldsymbol{\psi}_f(\phi) = \mathbf{I}_{n_c} \otimes \boldsymbol{\gamma}(\phi), \quad (18)$$

with $\boldsymbol{\gamma}(\phi)$ the basis for \mathbf{f}^\pm and \otimes the Kronecker product. In the current paper, commutation functions are defined by the following basis. Given a grid $\phi_\gamma \in \mathbb{R}^{n_\alpha}$ with rotor positions $\phi_{\gamma,i}$ spaced between 0 and $2\pi/n_t$, we define

$$\boldsymbol{\gamma}(\phi) = [k(\rho_1(\phi)), \dots, k(\rho_{n_\alpha}(\phi))], \quad (19)$$

where

$$\rho_i(\phi) = \frac{1}{\ell} \sqrt{(\mathbf{x}_{1,i} - \mathbf{x}_2(\phi))^\top (\mathbf{x}_{1,i} - \mathbf{x}_2(\phi))} \quad (20)$$

with length scale $\ell > 0$, and

$$\mathbf{x}_{1,i} = \begin{bmatrix} \sin(\phi_{\gamma,i} n_t) \\ \cos(\phi_{\gamma,i} n_t) \end{bmatrix}, \quad \mathbf{x}_2(\phi) = \begin{bmatrix} \sin(\phi n_t) \\ \cos(\phi n_t) \end{bmatrix}. \quad (21)$$

Moreover, the kernel function k in (19) is given by

$$\begin{aligned} k(\rho) &= \exp\left(-\sqrt{2\mu+1}\rho\right) \frac{\mu!}{(2\mu)!} \\ &\cdot \sum_{n=0}^{\mu} \frac{(\mu+n)!}{n!(\mu-n)!} \left(2\sqrt{2\mu+1}\rho\right)^{\mu-n}, \end{aligned} \quad (22)$$

This model structure draws inspiration from Gaussian Process (GP) regression, where k is recognized as a Matérn kernel. These choices are new in the design of commutation

functions. The kernel enforces periodicity and smoothness and is very successful in GP regression [3]. Specifically, (21) ensures that \mathbf{f}^\pm exhibits periodic behavior corresponding to the spatial period of a rotor tooth. Moreover, the designer can control the smoothness of \mathbf{f}^\pm by adjusting the length scale ℓ or the parameter $\mu \in \mathbb{N}$.

B. Torque ripple quantification in commutation design

The objective is designing $\mathbf{f}^\pm(\phi, \alpha)$ to minimize the expected torque ripple over all possible realizations of the random model $\hat{\mathbf{g}}$. To achieve this, we first define the estimated relative torque error $\hat{\varepsilon}^\pm(\phi, \theta, \alpha) \approx \varepsilon^\pm(\phi, \alpha)$ as

$$\begin{aligned}\hat{\varepsilon}_T^\pm(\phi, \theta, \alpha) &:= \hat{b}^\pm(\phi) \mp 1, \\ &= \hat{\mathbf{g}}(\phi, \theta) \mathbf{f}^\pm(\phi, \alpha) \mp 1.\end{aligned}\quad (23)$$

Substitution of (16) and (17) yields

$$\hat{\varepsilon}_T^\pm(\phi, \theta, \alpha) = \theta^\top \psi_g^\top(\phi) \psi_f(\phi) \alpha^\pm \mp 1. \quad (24)$$

For reasons that become apparent later, a vector $\hat{\varepsilon}_T$ is defined that stacks $\hat{\varepsilon}_T^\pm(\phi)$ as follows: where

$$\hat{\varepsilon}_T = [\hat{\varepsilon}_T^+(\phi_{\varepsilon,1}), \dots, \hat{\varepsilon}_T^+(\phi_{\varepsilon,N}), \hat{\varepsilon}_T^-(\phi_{\varepsilon,1}), \dots, \hat{\varepsilon}_T^-(\phi_{\varepsilon,N})]^\top. \quad (25)$$

Here, $\phi_\varepsilon \in \mathbb{R}^N$ is an evenly spaced grid of rotor angles $\phi_{\varepsilon,i}$ between 0 and $2\pi/n_t$. The expression for the vector $\hat{\varepsilon}_T$ of estimated torque errors is then given by

$$\hat{\varepsilon}_T = \mathbf{X}(\alpha) \theta + \begin{bmatrix} -\mathbf{1}_N \\ \mathbf{1}_N \end{bmatrix}, \quad (26)$$

with

$$\mathbf{X}(\alpha) = \mathbf{F}(\alpha) \Psi_g, \quad (27)$$

where $\Psi_g = \mathbf{1}_2 \otimes [\psi_g^\top(\phi_{\varepsilon,1}), \dots, \psi_g^\top(\phi_{\varepsilon,N})]^\top$ and

$$\mathbf{F}(\alpha) = \sum_{i=1}^{2N} \mathbf{E}_{ii} \otimes (\alpha^{\Omega_i} \psi_f^\top(\phi_{\varepsilon,i})), \quad (28)$$

$$\text{with } \Omega_i := \begin{cases} + & 1 \leq i \leq N, \\ - & N < i \leq 2N. \end{cases}$$

Here, $\mathbf{E}_{ii} \in \mathbb{B}^{2N \times 2N}$ denotes a matrix unit, which has only one nonzero entry at the i^{th} row and column.

In summary, (26) yields a vector $\hat{\varepsilon}_T$ of estimated torque errors, evaluated on a grid ϕ_ε . Since this vector is linear in the random SRM model parameters θ , see (14), we can write

$$\begin{aligned}\hat{\varepsilon}_T &\sim \mathcal{N}(\mu_\varepsilon, \Sigma_\varepsilon), \\ \mu_\varepsilon &= \mathbf{X}(\alpha) \hat{\theta} + \begin{bmatrix} -\mathbf{1}_N \\ \mathbf{1}_N \end{bmatrix}, \\ \Sigma_\varepsilon &= \mathbf{X}(\alpha) \Sigma_\theta \mathbf{X}^\top(\alpha).\end{aligned}\quad (29)$$

In this way, the estimated torque error is expressed in terms of the variance Σ_θ of the SRM model parameters θ . Two key observations can be made from (29). First, more uncertainty in the model parameters leads to a larger variance of $\hat{\varepsilon}_T$, i.e., potentially more torque ripple, even if α is designed such that $\hat{\varepsilon}_T$ is zero-mean. Second, the variance of $\hat{\varepsilon}_T$ is quadratically dependent on α , indicating that α can be tuned to obtain robust commutation functions $\mathbf{f}(\phi, \alpha)$ that have minimal variance Σ_ε of the expected torque ripple $\hat{\varepsilon}_T$. The next section describes how this can be achieved.

C. Optimization problem formulation

The objective is to find the optimal α that minimizes the expected torque ripple, $\hat{\varepsilon}_T$. The cost function, which penalizes the norm of the estimated torque ripple, is expressed using the approximation:

$$\begin{aligned}\tilde{\mathcal{J}}(\alpha) &= \|\hat{\varepsilon}_T^+(\phi, \theta, \alpha^+) \|_{2, \Phi'}^2 + \|\hat{\varepsilon}_T^-(\phi, \theta, \alpha^-) \|_{2, \Phi'}^2 \\ &= \int_0^{2\pi/n_t} (\hat{\varepsilon}_T^+(\phi, \theta, \alpha^+))^2 + (\hat{\varepsilon}_T^-(\phi, \theta, \alpha^-))^2 d\phi \\ &\approx \|\hat{\varepsilon}_T\|_2^2.\end{aligned}\quad (30)$$

Since $\hat{\varepsilon}_T$ is random, see (29), it follows that

$$\begin{aligned}\mathbb{E}[\tilde{\mathcal{J}}(\alpha)] &= \mathbb{E} \left[\hat{\varepsilon}_T^\top \hat{\varepsilon}_T \right], \\ &= \text{tr} \left(\mathbb{E} \left[\hat{\varepsilon}_T^\top \hat{\varepsilon}_T \right] \right) = \mathbb{E} \left[\text{tr} \left(\hat{\varepsilon}_T \hat{\varepsilon}_T^\top \right) \right] \\ &= \text{tr}(\Sigma_\varepsilon) + \mu_\varepsilon^\top \mu_\varepsilon, \\ &= \text{tr}(\mathbf{X}(\alpha) \Sigma_\theta \mathbf{X}^\top(\alpha)) + \hat{\theta}^\top \mathbf{X}^\top(\alpha) \mathbf{X}(\alpha) \hat{\theta} \\ &\quad - 2 \begin{bmatrix} -\mathbf{1}_N^\top & \mathbf{1}_N^\top \end{bmatrix} \mathbf{X}(\alpha) \hat{\theta} + 2N,\end{aligned}\quad (31)$$

see [12, Section 3.2b] for details. This results in a cost function that is quadratic in α , and convex since Σ_θ is positive definite. Moreover, to ensure that the designed commutation functions yield positive squared currents for all gridded rotor angles, the following constraints are defined:

$$\begin{aligned}[\mathbf{f}^+(\phi_{\varepsilon,1}, \alpha)^\top, \dots, \mathbf{f}^+(\phi_{\varepsilon,N}, \alpha)^\top, \\ \mathbf{f}^-(\phi_{\varepsilon,1}, \alpha)^\top, \dots, \mathbf{f}^-(\phi_{\varepsilon,N}, \alpha)^\top]^\top \geq \mathbf{0},\end{aligned}\quad (32)$$

which are expressed linearly in $\alpha = [\alpha^{+\top}, \alpha^{-\top}]^\top$ as

$$\mathbf{B} \alpha \geq \mathbf{0}, \quad (33)$$

where

$$\begin{aligned}\mathbf{B} &= \sum_{i=1}^{2N} ((\mathbf{e}_i \otimes \mathbf{I}_{n_c}) \otimes \iota_i) \otimes \gamma_f(\phi_{\varepsilon,i}), \\ \text{with } \iota_i &:= \begin{cases} [1, 0] & 1 \leq i \leq N, \\ [0, 1] & N < i \leq 2N. \end{cases}\end{aligned}\quad (34)$$

Here, $\mathbf{e}_i \in \mathbb{B}^{2N}$ denotes a unit vector that has only one nonzero entry at the i^{th} element. Finally, the convex optimization problem for robust design of commutation functions is posed as

$$\begin{aligned}\min_{\alpha} \quad & \tilde{\mathcal{J}}(\alpha), \\ \text{subject to} \quad & \mathbf{B} \alpha \geq \mathbf{0}.\end{aligned}\quad (35)$$

This problem with $2n_c n_\alpha$ design variables and $2n_c N$ linear constraints is readily solved with a convex solver, e.g., CasADi, see [13]. Note that in this framework, other terms can be easily included in the cost function and constraints, e.g., to mitigate power consumption, peak currents, maximum slew rates, or sampling-induced torque ripple [3].

In the next section, the effectiveness of the robust commutation functions in mitigating torque ripple from SRM-by-SRM manufacturing variations is demonstrated using Monte Carlo simulations.

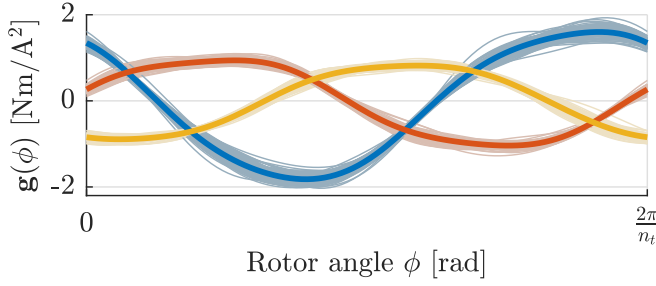


Fig. 3. Torque-current-angle relationships $\mathbf{g}(\phi, \theta_i)$ of the simulated SRMs, each of which is slightly different ($\lambda = 1$). The average $\mathbf{g}(\phi, \theta^\circ)$ is shown in bold.

IV. SIMULATION RESULTS

To demonstrate that the developed framework for robust design of commutation functions leads to improved tracking performance in the face of model mismatch, Monte Carlo simulations are carried out. First, the simulation setup is described, and subsequently, the conventional commutation functions used for comparison are described. Finally, the results are analyzed.

A. Simulation setup

A series of $M = 100$ different Switched Reluctance Motors is considered, each featuring $n_t = 131$ identical teeth and $n_c = 3$ coils. The linear continuous-time dynamics of each SRM are represented as:

$$G(s) := \frac{\phi(s)}{T(s)} = \frac{1}{s(s+1)}, \quad (36)$$

and a PID control $C(s)$ is designed to have a bandwidth of 20 Hz. The true nonlinear torque-current-angle relationship of the SRMs is given by

$$\mathbf{g}^\top(\phi, \theta_i) = \psi_g(\phi) \theta_i, \quad i \in \{1, \dots, M\}, \quad (37)$$

where the variation across the SRMs follows from

$$\theta_i \sim \mathcal{N}(\theta^\circ, \lambda \Sigma_\theta), \quad (38)$$

with $\lambda > 0$, $\theta \in \mathbb{R}^{90}$, and the structure ψ_g comprises of radial basis functions, see Figure 3.

The rotor angle ϕ is sampled at a rate of 5 kHz. At this rate, sampling-induced torque ripple is observed to be negligible at only 1% of the total torque ripple [3], i.e., the tracking error is approximately zero when a commutation function \mathbf{f}_i is designed to perfectly invert \mathbf{g}_i .

In this simulation study, the true systems \mathbf{g}_i are considered unknown, only a single probabilistic model $\hat{\mathbf{g}}$ is available with structure (16) and parameters $\theta \sim \mathcal{N}(\theta^\circ, \lambda \Sigma_\theta)$. This unbiased model is used to design one single commutation function \mathbf{f} , which is applied to each SRM. Because of the variation across SRMs, it is to be expected that each SRM will suffer from torque ripple.

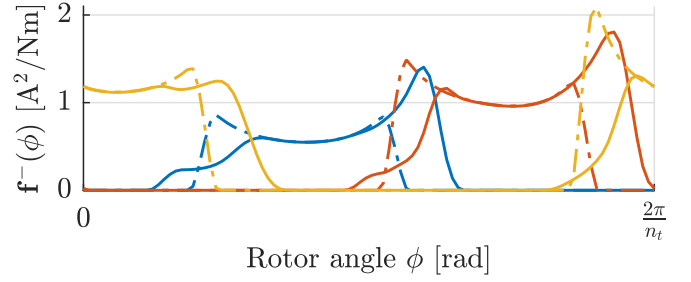


Fig. 4. The developed robust commutation functions \mathbf{f}^- (solid), designed to invert $\mathbb{E}[\mathbf{g}(\phi, \theta)]$, and conventional commutation functions $\mathbf{f}_{\text{conv}}^-$ (dot-dashed), designed to invert only the mean $\mathbf{g}(\phi, \theta^\circ)$. The developed commutation functions exhibit much more overlap, leading to careful switching of the currents in the face of model uncertainty.

B. Benchmark: conventional commutation functions

The performance of the developed robust commutation function \mathbf{f} is compared to the performance obtained using a commonly used conventional commutation function \mathbf{f}_{conv} . This function is given by

$$\mathbf{f}_{\text{conv},c}(\phi, T^*) = \mathbf{f}_{\text{TSF},c} \left(\phi + \frac{2\pi(c-1)}{n_c}, T^* \right) \cdot \text{sat}(1/\hat{g}_c(\phi, \theta^\circ)) T^*, \quad (39)$$

where $\mathbf{f}_{\text{conv},c}$ denotes the c^{th} element of \mathbf{f}_{conv} . Additionally, the saturation function $\text{sat}(x)$ is defined as:

$$\text{sat}(x) := \begin{cases} x_{\min} & x < x_{\min}, \\ x & x_{\min} \leq x \leq x_{\max}, \\ x_{\max} & x > x_{\max}. \end{cases} \quad (40)$$

Moreover, $\mathbf{f}_{\text{TSF}}(\phi, T^*) : \mathbb{R} \times \mathbb{R} \rightarrow \mathbb{R}^{n_c}$ represents a torque sharing function that distributes a desired torque to different coils while satisfying

$$\sum_{c=1}^{n_c} \mathbf{f}_{\text{TSF},c}(\phi, T^*) = \begin{cases} 1 & T^* \geq 0, \\ -1 & T^* < 0, \end{cases} \quad (41)$$

as detailed in [7]. Note that at values of ϕ where $g_c(\phi) = 0$, $\mathbf{f}_{\text{TSF},c}(\phi, T^*) = 0$ by design, ensuring that (39) is well defined for all ϕ .

C. Results and analysis

The developed framework is applied to design a single commutation function $\mathbf{f}(\phi, \alpha)$ based on the probabilistic model of $\mathbf{g}(\phi, \theta)$ with $\lambda = 1$ as follows. The commutation function \mathbf{f} is parametrized as in (5) and (17), with $n_\alpha = 50$, $\ell = 0.3$ and $\mu = 3$. Problem (35) is then posed for a grid of $N = 100$ points. This leads to an optimization problem with 300 design variables and 600 constraints. Using CasADi with MATLAB on a personal computer, the problem is parsed and solved in 300 s.

The resulting commutation function is shown in Figure 4. For brevity, the presentation of results focuses on \mathbf{f}^- , mostly omitting \mathbf{f}^+ . It can be seen that the commutation functions

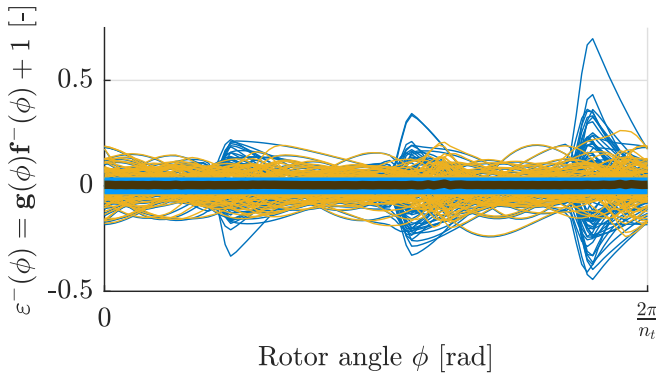


Fig. 5. Torque ripple of all SRMs. Commutation functions \mathbf{f}^- and \mathbf{f}_{conv} are designed to invert $\mathbf{g}(\phi, \theta^\circ)$, so the average torque ripple is expected to be low for both \mathbf{f}^- (—) and \mathbf{f}_{conv} (—). However, since each simulated SRM is slightly different with $\theta_i \neq \theta^\circ$, each SRM suffers from torque ripple. The developed robust commutation function \mathbf{f}^- leads to significantly less torque ripple (—) than the conventional functions \mathbf{f}_{conv} (—) because the model uncertainty is taken into account in the design phase.

\mathbf{f}^- exhibit significantly more overlap than \mathbf{f}_{conv} . This observation is interpreted as switching the currents carefully: near the rotor angles ϕ where the currents are switched to the next coil, a sharp change in current at a slightly incorrect angle would induce significant torque ripple. The conventional function \mathbf{f}_{conv} is designed purely for minimal power consumption given some constraints on the slope of the current and thus switches more abruptly, inducing torque ripple, as shown in more detail below.

To see how \mathbf{f} mitigates torque ripple, consider Figure 5. Both \mathbf{f} and \mathbf{f}_{conv} are designed to have approximately zero torque error for the nominal model $\hat{\mathbf{g}}(\phi, \theta^\circ)$. However, when an SRM with dynamics $\mathbf{g}(\phi, \theta_i)$ has parameters θ_i ever so slightly different from θ° , significant torque ripple occurs: up to 70%. Indeed, the torque ripple that follows from \mathbf{f} is significantly smaller in magnitude than the torque ripple resulting from \mathbf{f}_{conv} , indicating that the designed commutation functions truly are more robust to model uncertainty. Note that it is impossible in general to have zero torque error when $\hat{\mathbf{g}} \neq \mathbf{g}$, especially at angles ϕ where only one coil is magnetized.

To quantify the increase in tracking performance achieved by the robust commutation functions, four closed-loop simulations are carried out for all M SRMs. First, a reference is tracked with a constant velocity of 0.3 teeth/s for a duration of 5 teeth, using \mathbf{f}_{conv} . Next, the simulation is repeated using \mathbf{f} , and finally, both simulations are repeated in the other direction. The results are shown in Figure 6. The average RMS tracking error e_{RMS} is reduced significantly, see Table I, where

$$e_{\text{RMS}}^\pm := \sqrt{\frac{1}{N_f - N_s} \sum_{k=N_s}^{N_f} (e^\pm(t_k))^2}, \quad (42)$$

$$e_{\text{RMS}} := \sqrt{\frac{1}{2} ((e_{\text{RMS}}^+)^2 + (e_{\text{RMS}}^-)^2)},$$

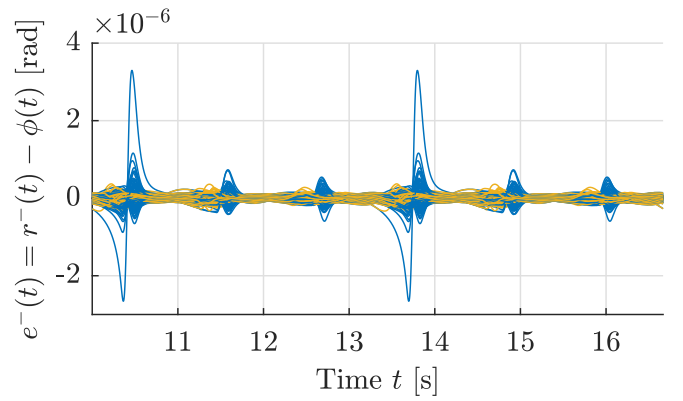


Fig. 6. Tracking error during the last two teeth, for all simulated SRMs in a constant velocity task. The designed commutation function \mathbf{f}^- results in less tracking error (—) than the conventional function \mathbf{f}_{conv} (—).

TABLE I
TRACKING PERFORMANCE OF ALL SIMULATED SRMs, $\lambda = 1$

	Conventional		Robust	
e_{RMS}^\pm [μrad]	Forwards	Backwards	Forwards	Backwards
Median	0.085	0.091	0.066 (-22%)	0.063 (-31%)
Average	0.093	0.100	0.068 (-27%)	0.065 (-35%)
Maximum	0.210	0.705	0.108 (-48%)	0.113 (-84%)

with N_s corresponding to the sample at which the rotor is at the second last tooth, and N_f the last sample.

Finally, it is investigated how the achieved performance relates to the magnitude λ of the variance, see (38). In this case, the same Monte Carlo setup is used, but λ is varied. For $\lambda = 0$, only one SRM with $\mathbf{g} = \mathbf{g}(\phi, \theta^\circ)$ is simulated, for all other values of λ , $M = 100$ and all θ are sampled from θ using the same random seed, such that $\theta_i = \theta^\circ + \lambda \Delta_{\theta,i}$. The results are shown in Figure 7. First, notice that for $\lambda = 0$, the conventional commutation functions lead to a smaller error. This is because \mathbf{f}_{conv} is parametrized in such a way that the torque ripple is exactly zero when the model is perfect, see (39). This is not the case for \mathbf{f}^\pm which is parametrized linearly in the parameters, see the bold lines in Figure 5. However, this is only a small price to be paid, since even a very small variance $\lambda = 0.1$ leads to a significant performance increase using the robust commutation functions, as seen in Figure 7. Moreover, for large modeling errors, the conventional commutation functions result in extremely large outliers for the tracking errors, while the developed commutation functions are much more robust to large model mismatches.

V. EXPERIMENTAL RESULTS

Modeling errors in the torque-current angle relationship of SRMs do not only arise from manufacturing variations across different SRMs but also variations across the teeth of one SRM. This section shows experimentally how the developed robust commutation functions mitigate the torque ripple resulting from such variations.

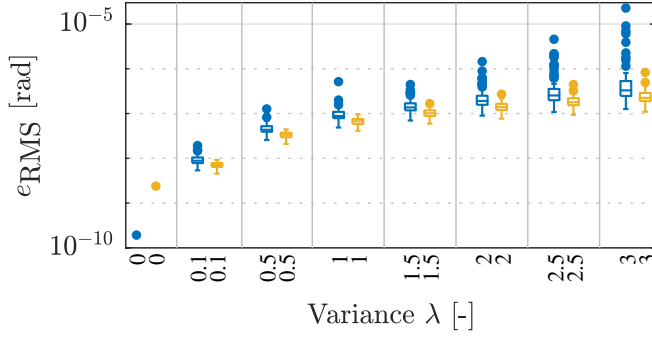


Fig. 7. RMS tracking error as a function of the variance λ . Higher values of λ indicate a more severe mismatch between the used model θ° and the true simulated SRM with parameters θ_i . The developed robust commutation functions \mathbf{f} result in a smaller error (orange) than the conventional functions \mathbf{f}_{conv} (blue) when even the slightest modeling errors are present.

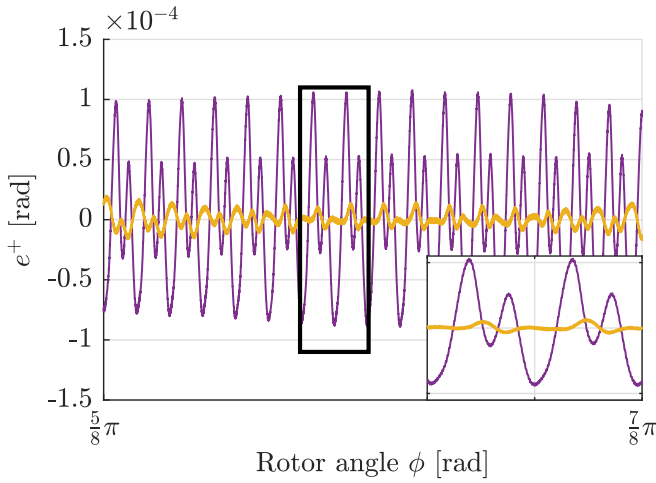


Fig. 8. Experimental data. Tracking error along a section of the rotor, showing considerable tooth-by-tooth variation. When using a simple model $\hat{\mathbf{g}}_{\text{sine}}$, the robust commutation function \mathbf{f} (E2, —) results in less tracking error than the conventional function \mathbf{f}_{conv} (E1, —). A similar improvement of the robust commutation functions (E4, —) with respect to conventional functions (E3, —) is seen for a model $\hat{\mathbf{g}}$ that is identified using experimental data.

A. Experimental setup and method

A single SRM is considered with $n_t = 131$ teeth and $n_c = 3$ coils, see [2]. A PID controller with a bandwidth of 20 Hz is given, and the sampling frequency is 10 kHz. Four constant-velocity tracking experiments are carried out with $\dot{r} = 15$ teeth per second for one rotation using the following commutation functions:

- E1: A conventional commutation function \mathbf{f}_{conv} is constructed based on a $\hat{\mathbf{g}}_{\text{sine}}$ that consists of three sinusoids, shifted 120° in phase.
- E2: A robust commutation function \mathbf{f} is constructed for this sinusoidal model. The variance is chosen as $\Sigma_\theta = 5 \cdot 10^{-3}I$ and a model structure is a Fourier basis with 5 harmonics.
- E3: A conventional commutation function \mathbf{f}_{conv} is constructed based on a $\hat{\mathbf{g}}$ which is identified using [10].
- E4: A robust commutation function \mathbf{f} is constructed for this

identified model. The variance Σ_θ thus follows from experimental data.

Both robust commutation functions are created by solving (35) using $n_\alpha = 50$, $\ell = 0.3$, $N = 100$ and $\mu = 3$. To disregard parasitical disturbances that do not relate to commutation, e.g., bearing imperfections, the tracking error is averaged out over 25 experiments, each a 2π offset.

B. Results and analysis

The resulting error is shown in Figure 8. Indeed, significant tooth-by-tooth variation is observed. While all commutation functions are designed for the ‘average tooth’, each tooth is significantly different from the average, and hence, torque ripple occurs during every tooth. The median RMS error per tooth is reduced from 54.6 to 50.0 μrad by the robust commutation function for the sinusoidal model (-8%) and from 15.4 to 13.7 μrad for the identified model (-11%). The reduced performance increase with respect to the simulation results in Table I may in part be explained by effects that were not present in the simulations. Namely, phenomena such as sensor noise and magnetic saturation contribute to torque ripple as well. Therefore, the increased performance gained by attenuating torque ripple caused by tooth-by-tooth variations might be partially obscured by such phenomena, which increase the RMS error for all commutation functions.

When the identification method of [10] is paired with the robust commutation functions of the current paper, a complete framework is obtained initially requires only a very simple sinusoidal model $\hat{\mathbf{g}}_{\text{sine}}$ (E1), which is used to identify an accurate random model $\hat{\mathbf{g}}$, and subsequently inverted using the method presented in the current paper to obtain an \mathbf{f} that results in low expected torque ripple (E4) for all realizations of the model, including the variance $\text{var}(\hat{\mathbf{g}})$ that follows from differences across teeth and SRMs. This full procedure requires no torque sensors and no physical modeling and yields a low-order, versatile commutation function that can be deployed to many manufactured SRMs of the same design, despite manufacturing variations.

VI. CONCLUSIONS AND FUTURE WORK

A framework is developed for the design of robust commutation functions, which serve as a universal driver that enables accurate closed-loop control of SRMs, even in the presence of significant unknown variations across rotor teeth or different SRMs. By exploiting the model variance of the identified torque-current-angle relationship, a commutation function is obtained that optimally switches current from one coil to the next, to mitigate the induced torque ripple when a tooth deviates from the nominal model due to manufacturing imperfections. The decrease in torque ripple with respect to conventional commutation functions is especially pronounced when the modeling error is large, but it is considerable even for small modeling errors, as evidenced by Monte Carlo simulations. Moreover, experimental results verify the validity of the approach. The

results are promising for low-cost applications in which a single driver is applied to many different systems, or when constraints on memory or modeling effort lead to the requirement of low-order commutation functions. The developed approach then serves as a low-cost solution to mitigate torque ripple, improving tracking performance and reducing acoustic noise.

Future research is required to explore bases for the commutation functions that feature even fewer parameters. Moreover, the cost function and constraints of the optimization problem may be reframed on a continuous domain, to overcome the approximation error introduced by discretization of the cost function.

VII. ACKNOWLEDGEMENTS

The authors would like to thank TNO, and in particular Lukas Kramer and Joost Peters, for the developments that have led to these results and for their help and support in carrying out the experiments reported in this paper.

REFERENCES

- [1] T. J. E. Miller, *Switched Reluctance Motors and Their Control*. London, England: Oxford University Press, 1993, vol. 31.
- [2] L. Kramer, J. Peters, R. Voorhoeve, G. Witvoet, and S. Kuiper, "Novel motorization axis for a Coarse Pointing Assembly in Optical Communication Systems," in *IFAC PapersOnLine*, vol. 53, no. 2. Elsevier Ltd, 2020, pp. 8426–8431.
- [3] M. van Meer, G. Witvoet, and T. Oomen, "Optimal commutation for switched reluctance motors using gaussian process regression," *IFAC-PapersOnLine*, vol. 55, no. 37, pp. 302–307, 2022, 2nd Modeling, Estimation and Control Conference MECC 2022.
- [4] A. Katalenic, "Control of reluctance actuators for high-precision positioning," Ph.D. dissertation, Eindhoven University of Technology, 2013.
- [5] Y. Boumaalif and H. Ouadi, "Accounting for magnetic saturation in designing a SRM speed controller for torque ripple minimization," *International Journal of Power Electronics and Drive Systems (IJPEDS)*, vol. 14, no. 1, p. 77, mar 2023. [Online]. Available: <https://ijpeds.iaescore.com/index.php/IJPEDS/article/view/22063>
- [6] X. D. Xue, K. W. Cheng, and S. L. Ho, "Optimization and evaluation of torque-sharing functions for torque ripple minimization in switched reluctance motor drives," *IEEE Transactions on Power Electronics*, vol. 24, no. 9, pp. 2076–2090, 2009.
- [7] J. J. Wang, "A common sharing method for current and flux-linkage control of switched reluctance motor," *Electric Power Systems Research*, vol. 131, pp. 19–30, 2016.
- [8] V. P. Vujicic, "Minimization of Torque Ripple and Copper Losses in Switched Reluctance Drive," *IEEE Transactions on Power Electronics*, vol. 27, no. 1, pp. 388–399, 2012.
- [9] N. Mooren, "Intelligent Mechatronics through Learning," Ph.D. dissertation, Eindhoven University of Technology, 2022.
- [10] M. van Meer, R. A. González, G. Witvoet, and T. Oomen, "Nonlinear Bayesian Identification for Motor Commutation : Applied to Switched Reluctance Motors," in *Proceedings of the 62nd IEEE Conference on Decision and Control*, Singapore, 2023 (accepted for publication).
- [11] C. Gan, J. Wu, Q. Sun, W. Kong, H. Li, and Y. Hu, "A Review on Machine Topologies and Control Techniques for Low-Noise Switched Reluctance Motors in Electric Vehicle Applications," *IEEE Access*, vol. 6, pp. 31 430–31 443, 2018.
- [12] A. Mathai and S. Provost, *Quadratic Forms in Random Variables: Theory and Applications*, 12 1992, vol. 87.
- [13] J. A. E. Andersson, J. Gillis, G. Horn, J. B. Rawlings, and M. Diehl, "CasADi – A software framework for nonlinear optimization and optimal control," *Mathematical Programming Computation*, vol. 11, no. 1, pp. 1–36, 2019.